Facies Structure and Quantitative Parameters of the Pleistocene Sediments of the Andean Submarine Margin

M. A. Levitan[a], *, T. N. Gelvi[a], and L. G. Domaratskaya[a]

*[a]Vernadsky Institute of Geochemistry and Analytical Chemistry, Russian Academy of Sciences,
ul. Kosygina 19, Moscow, 119991 Russia*

***e-mail: m-levitan@mail.ru**

Abstract—The lithological-facies zonality of the Neo- and Eopleistocene sediments from two main areas of the Andean submarine margin is described for the first time. Processing of corresponding maps and isopach schemes using A.B. Ronov's volumetric method made it possible to calculate the quantitative parameters of sedimentation for distinguished types of Pleistocene sediments. Terrigenous sedimentation predominated and was intensified during the Pleistocene. The accumulation of biogenic opal in form of diatom frustules was more intense in the Eopleistocene than in the Neopleistocene. This is related to the activation of the Peruvian upwelling caused by the upwelling of the Antarctic Intermediate Water.

INTRODUCTION

This paper continues a cycle of our works dedicated to the Pleistocene sediments from submarine margins of the World Ocean (Levitan et al., 2018a etc.). In this cycle, we consider separately the Neopleistocene, i.e., Middle and Late Pleistocene (Q_{2+3}, 0.01–0.80 Ma), and the Eopleistocene or Early Pleistocene (Q_1, 0.80–1.80 Ma according to the "old" scale (Gradstein et al., 2004).

The above-mentioned publications on the back-arc sedimentary basins of the active margins of the northern and western Pacific Ocean, as well as sedimentary basins of the Antarctic passive margin in the southwest are mainly based on the results of deep-sea drilling. In this paper, the evolution of the Pleistocene sedimentation in the sedimentary basin of the Andean-type active margin of the southeastern Pacific Ocean is described on the basis of four ODP legs.

MODERN SEDIMENTATION ENVIRONMENT

The Andean mobile belt extends from the north southward along the western margin of the South America for approximately 9 thou. km and reaches the largest width (about 750 km) in its middle part (Khain, 2001). The average altitude accounts for approximately 4000 m, with the highest peaks reaching almost 7000 m. The Andean belt is subdivided into three parts having different tectonics and geological evolution: the Northern, Central, and Southern Andes. The boundaries between them pass at approximately 5° N and 42° S, respectively. The largest Central segment consists of three sectors: northern, central, and southern, with boundaries at approximately 15° S and 30° S (Khain, 2001) (Figs. 1a, 1b).

All the segments differ in orography and climate. These differences have been well described using quantitative parameters in (Montgomery et al., 2001). In particular, most part of the northern sector of the Central Andes is weakly rugged, with zones of the highest altitudes occupying about 50% of area. At the same time, to the south and north of this zone, the highest-altitude regions account for no more than 10–15% in area. The topographic ruggedness mainly determines the annual amount of atmospheric precipitates and the erosion rate. It should be noted that the Andes experienced mountainous glaciation (especially in the southern part of the belt), and glaciers play an important role in the erosion of the highland Andes. The snow line is located at a height of approximately 5000 m in the northern Central Andes and declines to approximately 1000 m in the southern South Andes. Below the snow line, the erosion is mainly controlled by short and strong mountainous rivers that are fed by thawed waters of glaciers and rains. The Andes span several climatic belts (equatorial, subequatorial, tropical, subtropical, and moderate), each of which is characterized by peculiar weathering and erosion.

(a)
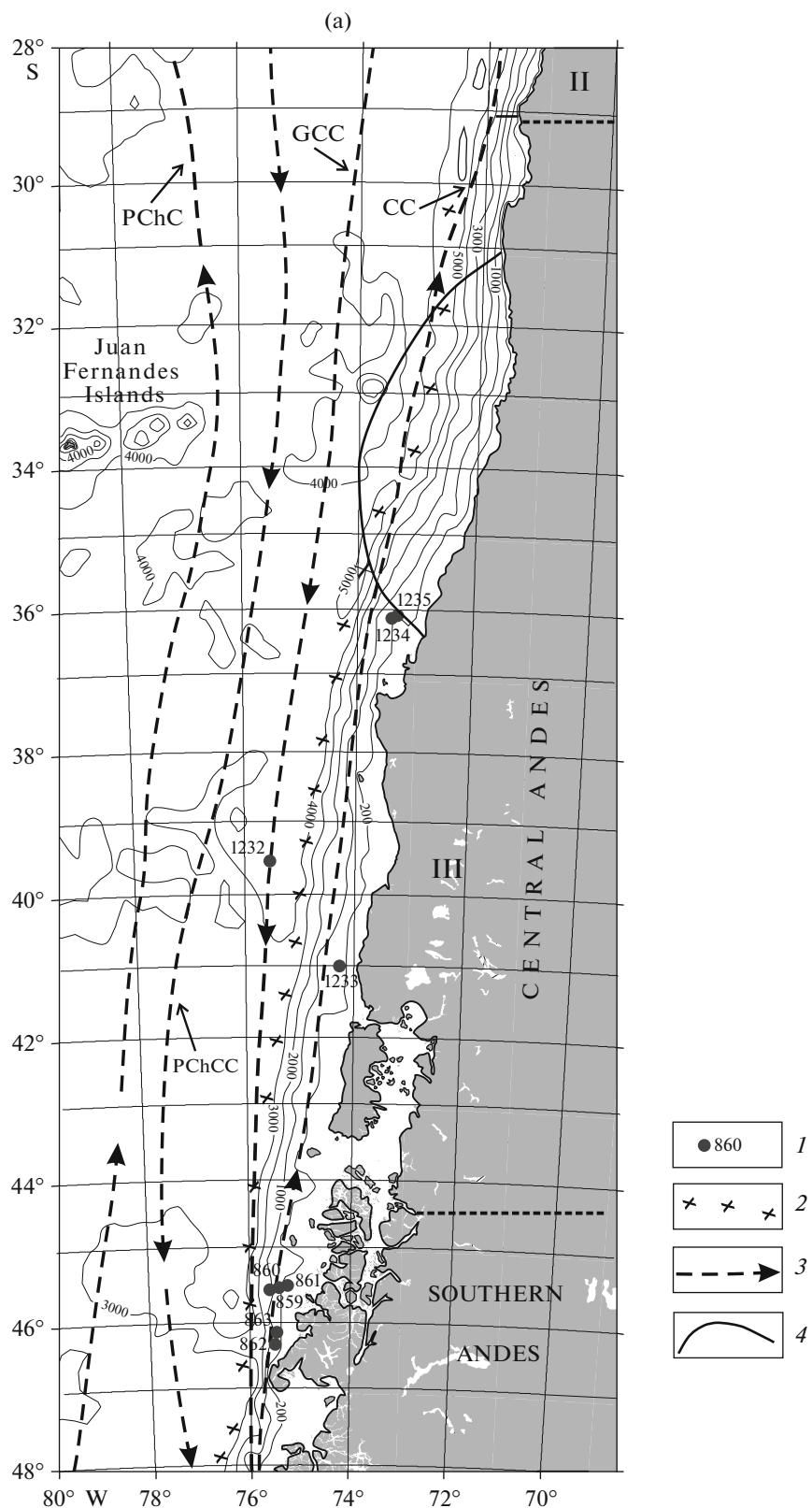
Fig. 1. Location of deep-water boreholes at the Andean submarine margin: (a) southern area and (b) northern area. Symbols: (*1*) deep-water holes; (*2*) deep-water Peruvian–Chilean trench; (*3*) surface currents; (*4*) upwelling boundaries. (PChC) Peruvian–Chilean current; (PChCC) Peruvian–Chilean countercurrent; (GCC) Gumboldt countercurrent; (CC) Coastal current (Mix et al., 2003). (I, II, III), northern, central, and southern sectors of the Central Andes (Khain, 2001). Isobaths are given in meters (www.gebco.org).
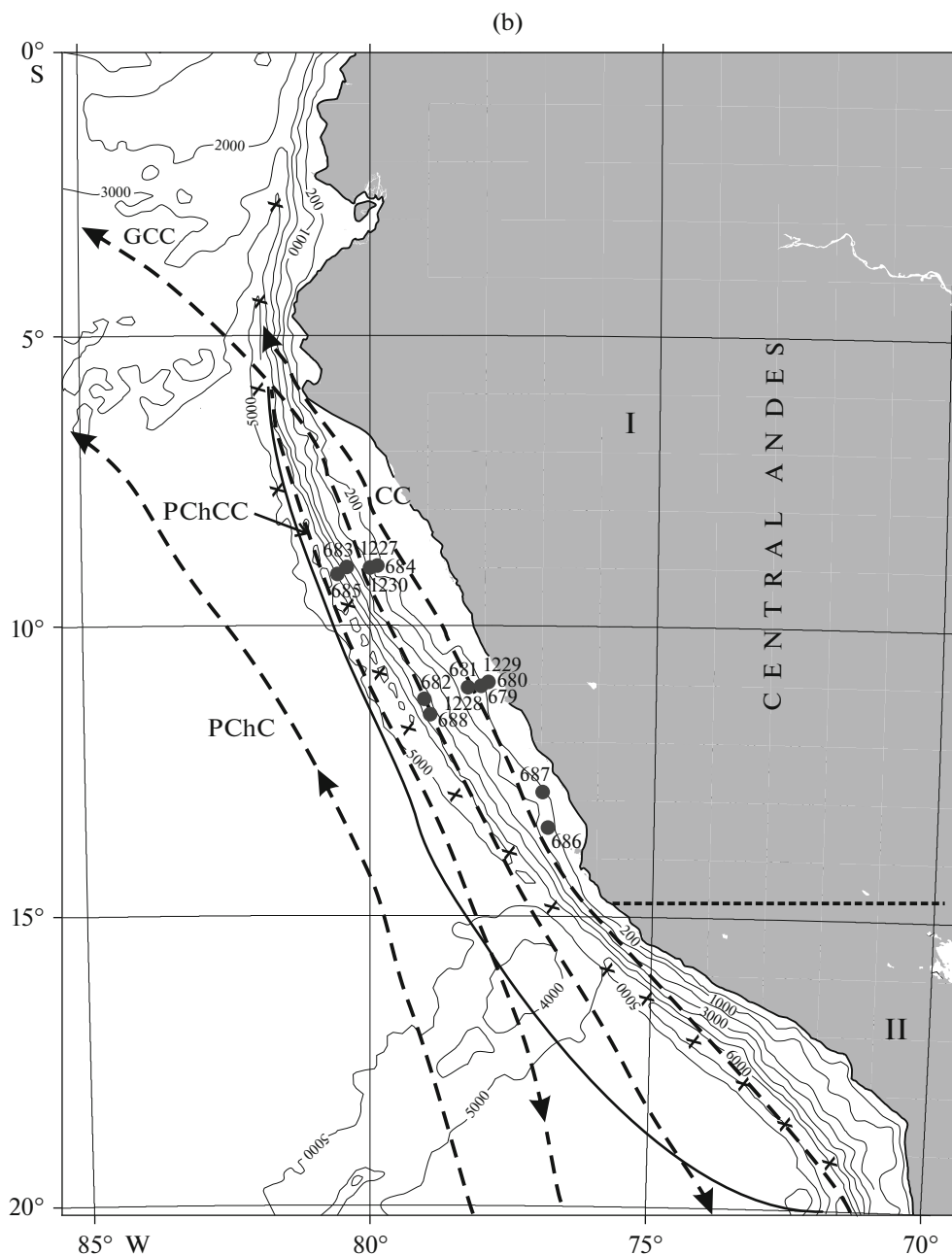
(b)

Fig. 1. (Contd.)

The Andean belt is one of the most active neotectonic belts, where the velocity of ascending orogenic movements reaches up to 2 mm/yr (Trifonov and Sokolov, 2015). This belt is also characterized by the high modern and Quaternary volcanic activity. All these processes provide a powerful lithogenic supply into the Pacific basin.

The coastal plain and continental shelf usually have insignificant total width (up to a few tens of kilometers). The steep Andean western slopes inclines at angles approximately corresponding to that of the continental slope descending to the Peruvian–Chilean deep-sea trench, with a thalweg located at depths of 5000–6000 m (Figs. 1a, 1b). In general, it should be noted that the Andean submarine margin is very narrow and frequently accounts for a few tens of kilometers wide, increasing locally to 150–200 km.

The annual temperature on the ocean surface in the studied region varies from 14°C in the south to 24°C in the equatorial part (Mix et al., 2003). The main currents are directed to the north (Peruvian–Chilean Current, Coastal Current) and south (Peru–

Chile Countercurrent and Humboldt Countercurrent) (Figs. 1a, 1b), alternating with each other. The vertical circulation in the water column is controlled by the atmospheric circulation: southern or southeastern winds in some areas form offshore currents, which moving westward make room for the ascent of the nutrient-rich Antarctic Intermediate Water. The areas of maximally expressed ascents are termed upwellings and expressed on the ocean surface, in particular, by the elevated contents of dissolved phosphates. There are two main upwellings: Chilean (concentration of dissolved phosphates is 0.6–0.8 µM) and more intense Peruvian (phosphate concentration reaches up to 1 µM) (Mix et al., 2003) ones (Figs. 1a, 1b).

The upwelling zones are characterized (especially, in summer) by extremely high primary production (about 300 g C/m^2 per yr) (Dukhova and Sapozhnikova, 2014), with formation of peculiar (upwelling) complexes of diatom algaes, benthic foraminifers, fishes, and others.

It should be noted that this part of the World Ocean is subjected to the periodic impact (with intervals from 4 to 9 years) of the *El Niño oscillation, which is* marked by a radical change of circulation systems and the development of the south-directed currents of the oxygen- and nutrient-rich warm and salt waters from equatorial–tropical area. This leads to the attenuation of southern winds up to their complete disappearance, termination of upwellings, stagnation in water column, fish die-off (Baturin, 1978), and intensification of storm activity.

As a result, the modern sediments of the surface layer in the described region are formed via mixing of lateral lithogenic (mainly terrigenous) fluxes and vertical diatom fluxes (McKoy et al., 2003). Upwelling sediments differ in the high contents of planktic organic matter, the abundance of authigenic phosphorites, glauconites, and iron sulfides (Baturin, 1978). At the same time, the Peruvian upwelling is much better expressed both in water column and in surface sediments than the Chilean upwelling. Seasonal manifestation of upwellings and El Nino leads to the well expressed banding (horizontal bedding) of bottom sediments.

FACTUAL MATERIAL AND METHODS

Four deep-sea drilling program legs have been carried out in the considered region: ODP legs 112 (Suess, von Huene et al., 1988), 141 (Behrmann et al., 1992), 201 (D'Hondt et al., 2003), and 202 (Mix et al., 2003). The location of drilled holes is shown in Figs. 1a, 1b. The lithological, stratigraphic, and physical properties of Pleistocene sediments were taken from cited deep-sea drilling reports.

Isobaths shown in Figs. 1a, 1b are from the General Bathymetric Chart of the World Ocean (www.gebco.org) published in 2004. The lithological map of the modern Pacific sediments was used for comparative–lithological analysis (McKoy et al., 2003). As in our previous works of this cycle, the comparative–lithological analysis was carried out using method by N.M. Strakhov (1945). The facies-genetic analysis was carried out using an approach by Murdmaa (1987), while volumetric method of map analysis was proposed by Ronov (1949). The sediment volume was recalculated into a dry sediment mass using formula from (Levitan et al., 2013). The Neo- and Eopleistocene lithological-facies maps were compiled using also boundaries between separate segments and sectors of the Andes shown in Figs. 1a, 1b.

RESULTS

The maps of factual material (Figs. 1a, 1b) and lithofacies maps with isopachs on a scale 1 : 10 000 000 were compiled for the Neo- and Eopleistocene time slices in the azimuthal equal-sized projection. Owing to the extremely large extension of the South America in submeridional direction and a relatively narrow width of its Pacific margin, all maps were made for two areas: southern (latitudinal boundaries from 48 to 28° S) and northern (latitudinal boundaries from 20° S to 0°). Therefore, the primary descriptions for these two areas will be given separately. No deep-sea drilling holes are available between these areas.

The Southern Andes

The Neopleistocene lithofacies map (Fig. 2a) shows the distribution of main sediment types on the submarine margin of the Southern Andes. It is seen that the most part of the map is occupied by a large field of hemipelagic clays, with the southernmost field (on the Southern Andes traverse) is made up of the alternation of hemipelagic clays, sands, and sandstones. The map also shows the field of terrigenous turbidites in the Chilean deep-water basin located beyond the deep-sea trench (hole 1232 data on), however data on turbidites were not involved in calculations with the Ronov volumetric method.

Hemipelagic clays are lithologically homogenous. This group also includes silty clays and clayey silts. Sometimes, the sediments contain small amounts of diatoms, foraminfers, and coccoliths, but the $CaCO_3$ content never exceeds a few percents. The hemipelagic clay sequence contains scarce thin intercalations of terrigenous turbidites and tephra. These rocks reveal no any traces of upwelling: the Corg content usually is less than 0.3% (more frequently lower than 0.1%) (Behrmann et al., 1992). Special studies showed that the geochemistry of hemipelagic clays is completely determined by the chemical composition of rock complexes of the corresponding Andean segment (Phanerozoic sedimentary rocks, Cretaceous batholiths, and Quaternary volcanics) (Kilian and Behrmann, 2003). Indeed, the hemipelagic clays exhibit definite

(a)
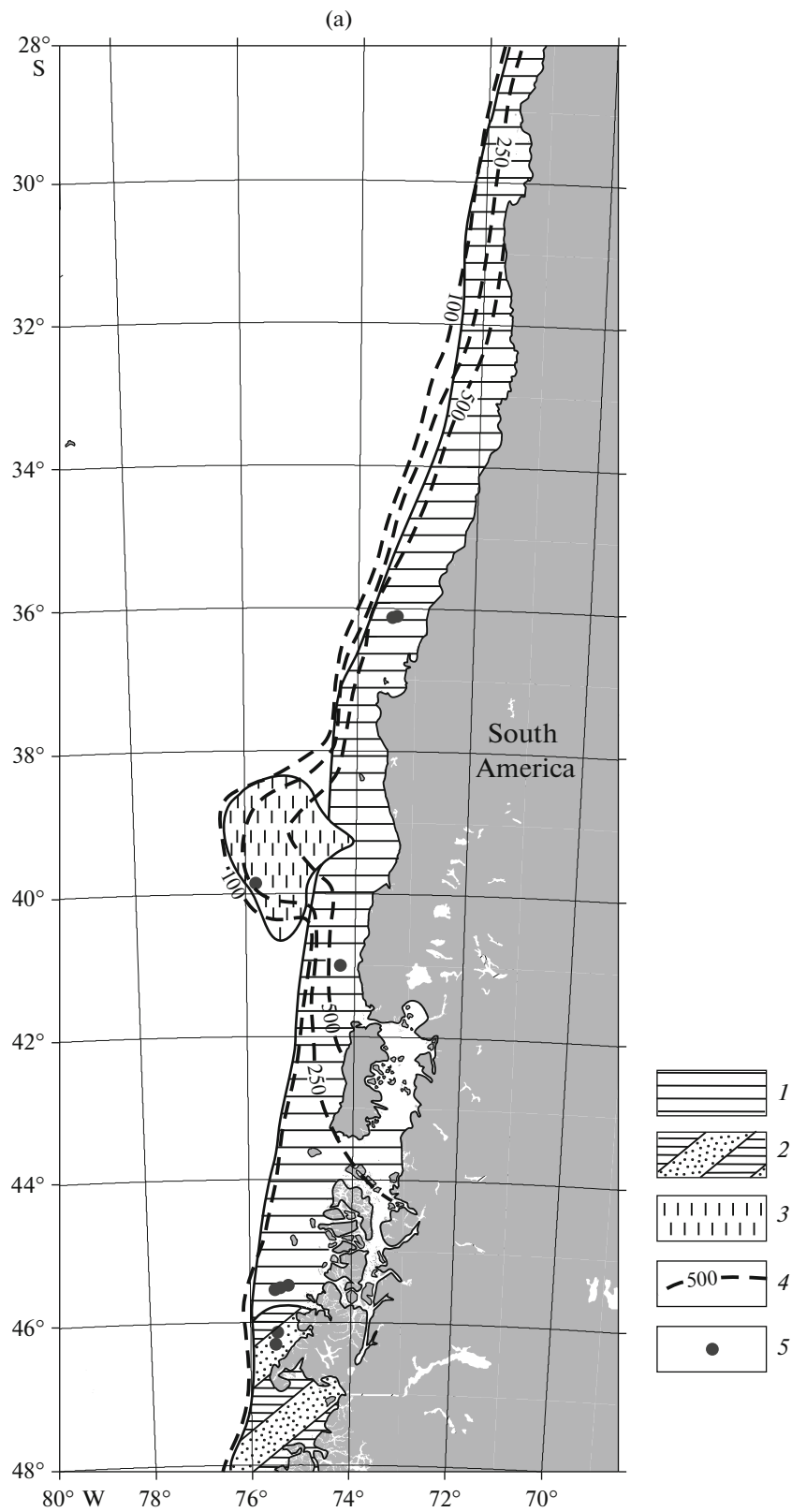
Fig. 2. Pleistocene lithological-facies map of the southern area: (a) Neopleistocene, (b) Eopleistocene. Symbols: (*1*) hemipe-lagic clays; (*2*) alternation of hemipelagic clays, sands, and sandstones; (*3*) terrigenous turbidites; (*4*) isopachs (m); (*5*) deep-water holes.
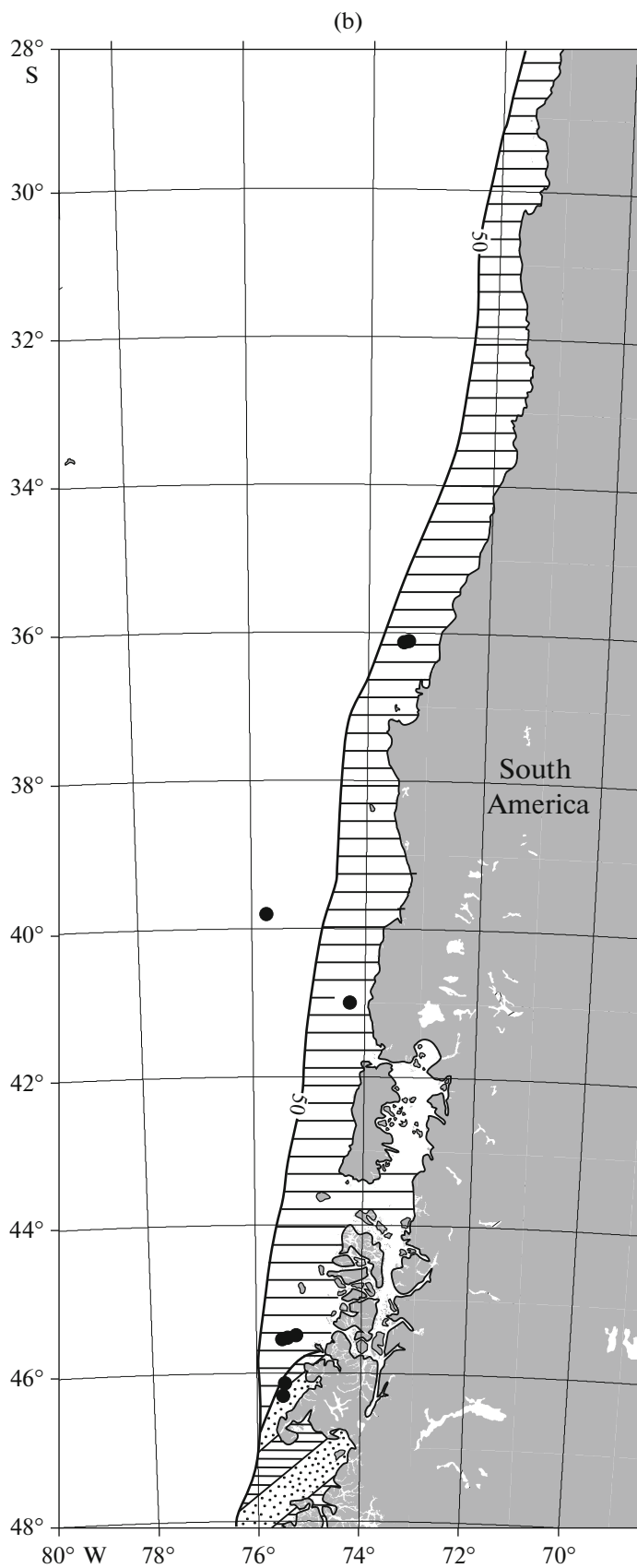
Fig. 2. (Contd.)

chemical variations along the strike of the belt in compliance with a change of petrographic composition of provenances (Lamy et al., 1998). For instance, hole 859 core has elevated contents of volcanogenic material.

The field of alternation of hemipelagic clays with sands and sandstones in the extreme south of the studied area reflects the transition of Central to Southern Andes on the land, with corresponding changes in the geological structure, Quaternary geological history, and denudation rates.

The aforementioned turbidite field was shown because turbid currents in this area were ejected beyond the limits of continental margin. This is related to the periodical disappearance of the trench on the floor surface due to the undulation of the deep-sea trench floor along strike. In this part, the turbid currents escape the natural sedimentation trap and could spread beyond the active margin.

The arrangement of isopachs of Neopleistocene sediments (Fig. 2a) is controlled by terrigenous sedimentation with the avalanche rates and a centrifugal decrease of thickness from sources areas to the pelagic zone. The linear extrapolation of sedimentation rates in the holes most close to the Central Andes on the continental slope showed the accumulation of giant sedimentary sequences (locally >1 km thick) during the Neopleistocene (sediments a few hundreds of meters thick and with age >0.26 Ma were recovered in the bottom of holes 1233−1235). A 100-m isopach usually does not go beyond the continental slope. The exception is only the mentioned turbidite field. In general, the sedimentation area is 213.00 thou. km^2, while the total volume of the sediments is 75.18 thou. km^3. The hemipelagic clays account for 97% of the total volume of sedimentary cover (Table 1).

The Eopleistocene lithofacies map (Fig. 2b) in general is identical to the Neopleistocene map (except for the turbidite field, since hole 1232 recovered sediments of only Neopleistocene age). However, there is one sharp difference, which consists in the much lower accumulation rate in the Eopleistocene. In all studied holes, the thickness of the Eopleistocene sequences varies from 50 to 100 m thick (Fig. 2b). It is noteworthy that the Chilean upwelling sediments shown in the map of the surface sediment layer of the Pacific Ocean (McKoy et al., 2003) have not been accumulated in the Neopleistocene and Eopleistocene.

The recalculation of sediment volumes (Table 1) for dry sediment mass and, further, for mass of sediments per time unit (Table 2) allowed us to unravel interesting trends in the evolution of the Pleistocene sedimentation in the southern part of the submarine Andean margin. In particular, it was revealed that the intensity of sedimentation in the Neopleistocene was higher than in the Eopleistocene: by 6.4 times for hemipelagic clays, 1.6 times for sands and sandstones, and 5.6 times for terrigenous sediments.

Table 1. Areas (S, thou. km^2) and volumes (V, thou. km^3) of main types of bottom sediments in the Neopleistocene and Eopleistocene ("southern" area)

Bottom sediments	Neopleistocene		Eopleistocene	
	S	V	S	V
Hemipelagic clays	213.00	73.05	221.50	11.42
Sandstones	24.25	2.13	24.00	1.54

Table 2. Mass of dry sediment (M, 10^{18} g) and mass of sediment per time unit (I, 10^{18} g/Ma) of main types of bottom sediments in the Neopleistocene and Eopleistocenee ("southern" map)
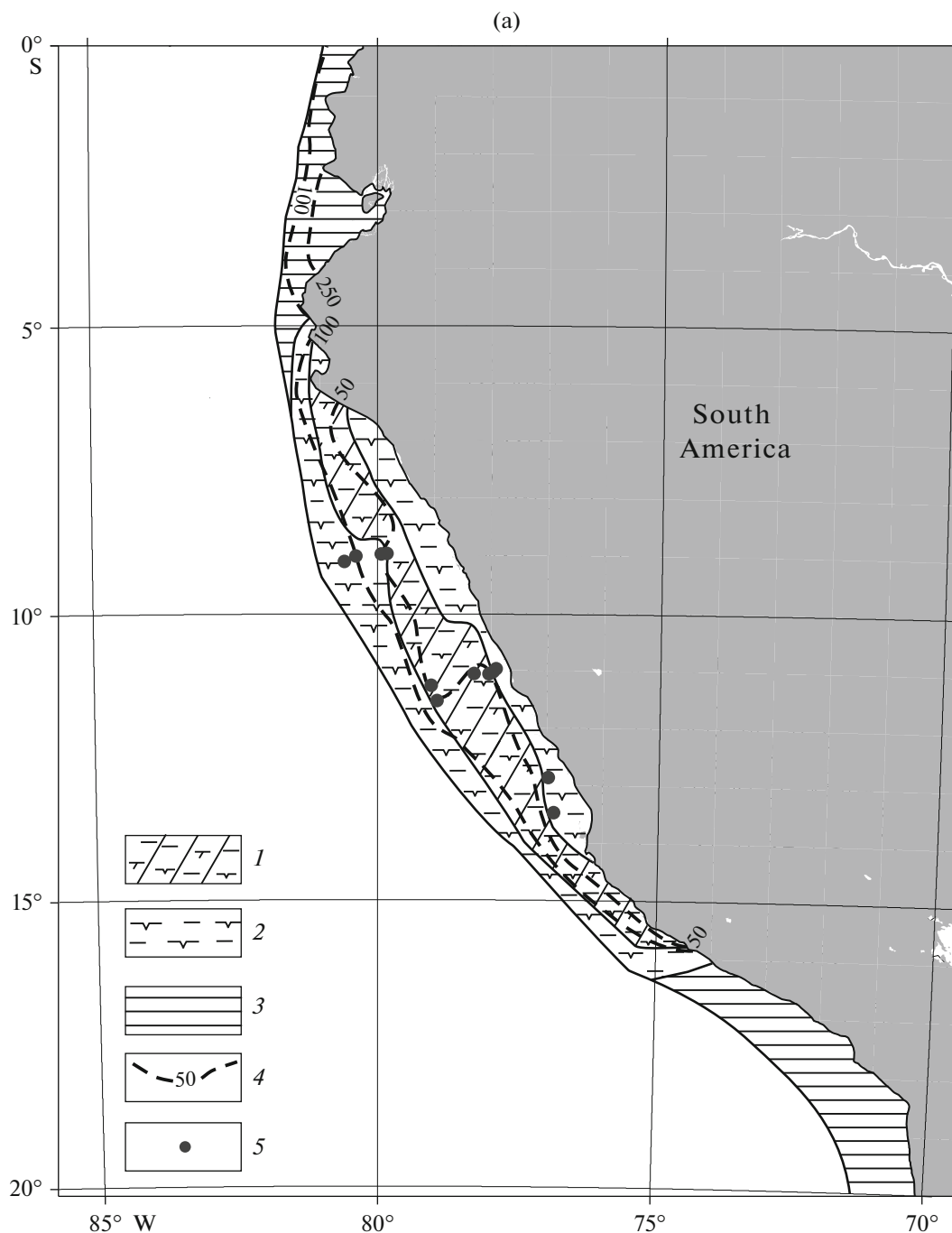
Bottom sediments	Neopleistocene		Eopleistocene	
	M	I	M	I
Hemipelagic clays	72.3	91.5	14.4	14.4
Sandstones	3.2	4.1	2.6	2.6

The Northern Area

The Neopleistocene lithofacies map (Fig. 3a) shows the distribution of main sediment types on the submarine margin of the Northern Andes. It is seen that hemipelagic clays are developed north of 5° S and south of 15° S (>33% of area), while the intervening area is occupied by diatom clay (>36% area) and diatom ooze−foraminiferal clays alternation (about 30% of the total area) (Table 2a). Thereby, sediments enriched in foraminifers are restricted to the shelf and the upper part of the continental slope. There are also less common shelf foraminiferal sands, and single thin intercalations of terrigenous sands, turbidites, and tephra. It should be noted that the northern and southern fields of hemipelagic clays are only inferred, because holes are absent there.

In general, this area demonstrates the well-expressed influence of the Peruvian upwelling: sediments from the central part of the area are enriched in Corg, phosphorite nodules, dolomites, pyrite, glauconite; contain peculiar assemblages of benthic foraminifers and diatoms; and intercalations enriched in fish bones.

It is seen from the distribution of isopachs of the Neopleistocene sediments (Fig. 3a) that thicknesses in the upwelling influence zone increase from the coast to the pelagic zone: gradation less than 50 m occupies the shelf and upper portions of continental slope; the gradation from 50 to 100 m occupies mainly the middle part of the slope; and >100 m, the lower part of the continental slope. Owing to the absence of holes, the accurate distribution of isopachs in the north and south is unknown. This problem will be considered in more detail below, in section "Discussion". The total area of sediments accounts for 343.7 thou. km^2, while their volume is 30.5 thou. km^3. Thereby, the relative

(a)

Fig. 3. Lithological-facies maps of Pleistocene sediments of the northern area. (a) Neopleistocene. Symbols: (*1*) alternation of foraminiferal and diatom clays; (*2*) diatom clays; (*3*) hemipelagic clays; (*4*) isopachs (m); (*5*) deep-water holes. (b) Eopleistocene. Symbols: (*1*) diatom ooze; (*2*) alternation of diatom clays, diatom ooze, and sands; (*3*) alternation of foraminiferal-diatom clays and diatom ooze; (*4*) hemipelagic clays; (*5*) foraminferal clays; (*6*) diatom clays; (*7*) isopachs (m); (*8*) deep-water holes.

input of diatom clays, hemipelagic clays, and diatom ooze in the total volume of the Neopleistocene sediments is 42.0, 38.4, 5.9%, respectively (Table 3).

The Eopleistocene lithofacies map (Fig. 3b) has much in common with the Neopleistocene map: the continental margin in the southern and northern parts of the area is occupied by hemipelagic clays (36.8% of total area, Table 3), while its central part is made up of diatom clays (53.6%) and intercalating diatom ooze, diatom and foraminferal clays (<10%). There are also single thin intercalations of tephra, terrigenous turbidites, and terrigenous sands. In general, the Eopleistocene lithogenetic types of sediments are lithologically very similar to the Neopleistocene sediments.
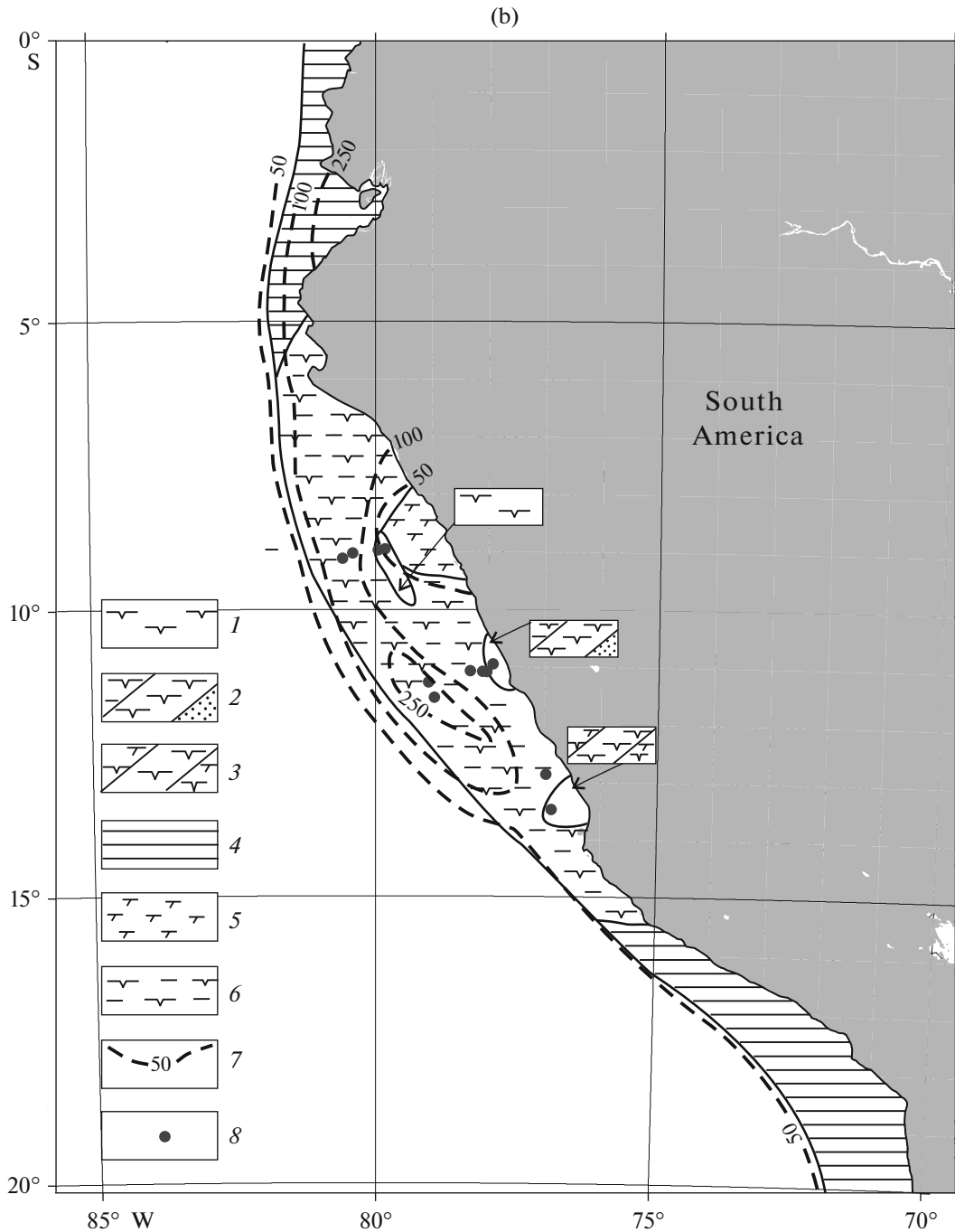
Fig. 3. (Contd.)

The distribution of isopachs for the Eopleistocene sediments also resembles the Neopleistocene scheme, however, in general their thicknesses increase: in the central part at the preservation of increasing trend from the coast to the pelagic zone, a 250-m isopach is noted in the lower parts of the continental slope. Correspondingly, the volumes of sediments significantly changed. Of the total volume of 53.4 thou. km³, diatom clays account for 53.6%, hemipelagic clays,

49.3%, diatom ooze, 1.8%, and foraminferal sediments, 0.7% (Table 3).

Recalculation of sediment volumes to dry sediment mass and mass of sediments per time unit (Table 4) showed that the main types of sediments (both hemipelagic and diatom clays) were accumulated in the Eopleistocene in much more amounts than in the Neopleistocene. Based on the fact that diatom clays contain on average 40% biogenic opal and 60% terrig-

Table 3. Areas (S, thou. km^2) and volume (V, thou. km^3) of main types of bottom sediments in the Neopleistocenee and Eopleistocenee ("northern" map)

Bottom sediments	Neopleistocene		Eopleistocene	
	S	V	S	V
Hemipelagic clays	114.6	11.7	130.6	26.3
Diatom clays	229.1	17.0	197.5	25.7
Diatom ooze	–	–	17.2	1.0
Foraminiferal sediments	104.6	1.8	16.1	0.4

Table 4. Mass of dry sediment (M, 10^{18} g) and mass of sediments per time unit (I, 10^{18} g/Ma) ("northern" map)

Bottom sediments	Neopleistocene		Eopleistocene	
	M	I	M	I
Hemipelagic clays	11.6	14.7	33.1	33.1
Diatom clays	7.4	9.4	11.2	11.2
Diatom ooze	–	–	0.4	0.4
Foraminiferal sediments	0.8	1.0	0.2	0.2

enous (more exactly, lithogenic one) matter (Gersonde et al., 2012), the intensity of accumulation of terrigenous matter in the Eopleistocene was higher than in the Neopleistocene: the IQ_{2+3}/IQ_1 ratio is 0.51. The corresponding ratio for biogenic opal represented by diatom frustules is 0.78.

Andean Submarine Margin

A comparative analysis of Tables 2 and 4 indicates that terrigenous sedimentation in the southern area was much more intense than in the northern area, while biogenic silica accumulation (unlike the northern area) was absent. Thereby, terrigenous sediments in the southern area were accumulated more rapidly in the Neopleistocene, while those in the northern area, in the Eopleistocene.

The comparison of the intensity of terrigenous accumulation in the Neopleistocene and Eopleistocene for the entire Andean submarine margin (in total, for the southern and northern areas) yields $IQ_{2+3}/IQ_1 = 2.0$, thus indicating an increase of intensity of terrigenous accumulation in the Pleistocene.

DISCUSSION

Above data indicate that the lithological composition of sediments of the Andean submarine margin in the Pleistocene, as in the modern epoch, was determined by proportions of terrigenous and biogenic (essentially diatom) fluxes. Thereby, the terrigenous material in general predominates over biogenic one.

The main source of terrigenous sediments was Andes. No accretionary wedges made up mainly of pelagic material were found on the continental slope. Special lithological studies of some holes revealed the presence of sedimentary material of mountainous glaciers, which in the snow line area was entrapped by fluvial flows and then was transported into the final sedimentation basin (Mix et al., 2003).

The distribution of terrigenous sediments along the Andean continental margins reflects both petrographic composition of provenances and the denudation rates of corresponding segments and sectors of this mountainous belt. A northward transition from a zone of hemipelagic clay–sand intercalation to a zone monofacies hemipelagic clays in the southern area reflected a transition from the Southern Andes to the Central Andes. This transition was associated with an increase of sedimentation rate. In the northern area, according to our considerations, the predominance of hemipelagic clays at the extreme south and north was caused by the absence of the Peruvian upwelling and by an increase of denudation rates of the Andes at the traverse of these zones owing to the highly rugged topography (Montgomery et al., 2001).

A decrease of sedimentation rates in the central part of the northern region was mainly related to the decrease of the terrigenous mass accumulation rates.

In our opinion, the above described centrifugal distribution of thicknesses of terrigenous sediments and an increase of sedimentation intensity in the Neopleistocene as compared to the Eopleistocene in the southern area is related to the neotectonic history of the adjacent Andean parts rather than to the evolution of mountainous glaciations in the Pleistocene. It is known that the scales of mountainous glaciations of the Andes were approximately identical in the first half of the Eopleistocene and in the second half of the Neopleistocene, and became slightly lower during the Middle Pleistocene transition (Clapperton, 1993).

It is obvious that a decrease of terrigenous mass accumulation intensity in the northern area in the Neopleistocene as compared to the Eopleistocene was caused by the different history of neotectonic movements in the adjacent Andean areas as compared to the southern area. However, the interpretation of observed thickness distribution of Pleistocene sediments across the strike of continental margin in the northern area remains still ambiguous. This could be related to a decrease of hydrodynamic activity in the nepheloid layer from shelf downward the continental slope for an unclear reason.

An alternative explanation is the existence of the Chilean upwelling with precipitation depocenter in the lower continental slope (as follows from the distribution of sediment thicknesses). Thereby, it is necessary to assume that the main mechanism of terrigenous supply in this zone is biotransport, i.e., the entrapment of terrigenous particles by organic matter

in the surface layers of water column, biosorption, bio-accumulation, biofiltration, and faecal transport during the precipitation of organic particles on the floor. This explanation seems to be more correct than "hydrodynamic" version.

The same mechanisms for the distribution of terrigenous material on the floor can be assumed for the northern and southern parts of the northern area.

Surface currents shown in Figs. 1a and 1b provided meridional redistribution of relatively insignificant part of marine suspended matter, which did not affect significantly on the thickness distribution. The donwslope lateral fluxes, first of all, in the nepheloid layer played the greater role.

The absence of upwelling traces in the sediments of the southern area is rather explained by the fact that the Chilean upwelling did not exist in the Pleistocene and appeared only in the Holocene. A clear activation of the Peruvian upwelling in the Eopleistocene as compared to the Neopleistocene additionally emphasizes its relation with the Antarctic Intermediate Water, since the Southern Ocean in the Ross Sea area is characterized by the predominance of silica accumulation in the Eopleistocene as compared to the Neopleistocene (Levitan et al., 2018b). Both these phenomena confirm the concept of two oceans: "ice and "non-ice" (Levitan, 2016).

The general consideration of the Andes demonstrates an obvious intensification of terrigenous accumulation on their submarine margin in the Neopleistocene as compared to the Eopleistocene, which coincides with a general trend for the Pacific pelagic areas (Levitan et al., 2013).

CONCLUSIONS

Two areas were distinguished along the submarine Andean margin: southern (with latitudinal boundaries from 48° to 28° S) and northern (from 20° S to 0°) ones. The former is characterized by only terrigenous sedimentation with a decrease of thickness from coast to the pelagic zone and an increase of terrigenous mass accumulation intensity in the Neopleistocene as compared to the Eopleistocene.

The central part of the northern area is occupied by sediments formed by the Peruvian upwelling, mainly, by diatom clays, and, to lesser extent, diatom oozes, foraminiferal clays, foraminiferal sands, and other sediments. Depocenter (an area of maximum deposition) in this area is restricted to the lower continental slope, while thickness decreases to the coast. This phenomenon is rather related to the position of upwelling in the Pleistocene and to the biotransport as the main mechanism of terrigenous sedimentation. Unlike the southern area, this area was characterized by a decrease of intensity of terrigenous sedimentation from the Eopleistocene to the Neopleistocene. The same tendency is typical of accumulation of biogenic

siliceous sediments. This is related to the relationship between this upwelling and the Antarctic Intermediate Waters. The Chilean upwelling in the Pleistocene did not exist.

In general, the submarine Andean margin demonstrates a strong influence of geological structure, topography, neotectonic activity, and the rate of land denudation on the composition, thickness distribution, and the Pleistocene evolution of terrigenous accumulation in the sedimentation basin.

As a result, the intensity of terrigenous accumulation on this margin was higher in the Neopleistocene than in the Eopleistocene, which coincides with the trend for the Pacific pelagic area (Levitan et al., 2013).

REFERENCES

G. N. Baturin, *Ocean-Floor Phosphorites* (Nauka, Moscow, 1978) [in Russian].

J. H. Behrmann, S. D. Lewis, R. J. Musgrave, et al., Proc. ODP, Init. Repts. **141**, (1992).

C. M. Clapperton, *Quaternary Geology and Geomorphology of South America* (Elsevier, Amsterdam, 1993).

S. L. D'Hondt, B. B. Jørgensen, D. J. Miller, et al., Proc. ODP, Init. Repts. **201**, (2003).

L. A. Dukhova and V. V. Sapozhnikov, "Hydrochemical indicators of primary production in zones of Peruvian and Canary upwellings," Tr. VNIRO **152**, 85−100 (2014).

R. Gersonde, "The expedition of the research vessel "Sonne" to the subpolar north Pacific and the Bering Sea in 2009 (SO202−INOPEX)," Ber. Polarforsch. **643**, (2012).

F. M. Gradstein J. G. Ogg, Smith A.G. et al., *A Geologic Time Scale 2004* (Cambridge Univ. Press, 2004).

V. E. Khain, *Tectonics of Continents and Oceans* (Nauchnyi Mir, Moscow, 2001) [in Russian].

R. Kilian and J. H. Behrmann, "Geochemical constraints on the sources of South Chile Trench sediments and their recycling in arc magmas of the Southern Andes," J. Geol. Soc. London **160**, 57−70 (2003).

F. Lamy, D. Hebbeln, and G. Wefer, "Terrigenous sediment supply along the Chilean continental margin: modern region patterns of texture and composition," Geol. Rundsch. **87**, 477−494 (1998).

M. A. Levitan, "Comparative analysis of pelagic Pleistocene silica accumulation in the Pacific and Indian oceans," Geochem. Int. **54** (3), 257−265 (2016).

M. A. Levitan, A. N. Balukhovsky, T. A. Antonova, and T. N. Gelvi, "Quantitative parameters of Pleistocene pelagic sedimentation in the Pacific ocean," Geochem. Int. **51**(5), 345−352 (2013).

M. A. Levitan, T. N. Gelvi, K. V. Syromyatnikov, and K. D. Chekan, "Facies structure and quantitative parameters of Pleistocene sediments of the Bering Sea," Geochem. Int. **56**(4), 304−317 (2018a).

M. A. Levitan, T. N. Gelvi, and L. G. Domaratskaya, "Facies structure and quantitative parameters of Pleistocene sediments of underwater continental margins of the Wilkes Land and Ross Sea, Antarctica," Vestn. Inst. Geol. Komi Center Ural. Otd. Ross. Akad. Nauk, No. 10, 17−22 (2018b).

F. W. McCoy, T. R. Swint, and D. Z. Piper, "Types of bottom sediments," *International Geological−Geophysical Atlas of the Pacific Ocean,* Ed. by G.B. Udinstev (Inyergovernmental Oceanographic Commission, Moscow−St. Petersburg, 2003), pp. 114−115.

A. C. Mix, R. Tiedemann, P. Blum, et al., Proc. ODP, Init. Repts. **202**, (2003).

D. R. Montgomery, G. Balco, and S. D. Willett, "Climate, tectonics, and the morphology of the Andes," Geology **29** (7), 579−582 (2001).

I. O. Murdmaa, *Ocean Facies* (Nauka, Moscow, 1987) [in Russian].

A. B. Ronov, *History of Sedimentation and Fluctuations of the European USSR: Volumetric Method Data,* Tr. Geofiz. Inst. Akad. Nauk SSSR, No. 3, (1949).

N. M. Strakhov, "Comparative−lithological direction and its tasks," Byull. Mosk. O-va. Ispyt. Prir., Otd. Geol. **20** (3/4), 34−48 (1945).

E. R. Suess, von Huene, et al., *Proc. ODP,* Init. Repts., **112**, (1988).

V. G. Trifonov and S. Yu. Sokolov, "On the way to post-plate tectonics," Vestn. Ross. Akad. Nauk **85**(7), 605−615 (2015).

www.gebco.org (2004)

Translated by M. Bogina